J Neurophysiol 103: 858–874, 2010.
First published December 9, 2009; doi:10.1152/jn.00099.2009.

Representation of Horizontal Head-on-Body Position in the Primate Superior Colliculus

Benjamin Nagy[1,2] and Brian D. Corneil[1,2,3]

[1]*Canadian Institutes of Health Research Group in Action and Perception,* [2]*Graduate Program in Neuroscience, and* [3]*Department of Physiology and Pharmacology and Department of Psychology, University of Western Ontario, London, Ontario, Canada*

Submitted 2 February 2009; accepted in final form 2 December 2009

Nagy B, Corneil BD. Representation of horizontal head-on-body position in the primate superior colliculus. *J Neurophysiol* 103: 858–874, 2010. First published December 9, 2009; doi:10.1152/jn.00099.2009. Movement-related activity within the superior colliculus (SC) represents the desired displacement of an impending gaze shift. This representation must ultimately be transformed into position-based reference frames appropriate for coordinated eye–head gaze shifts. Parietal areas that project to the SC are modulated by the initial position of both the eye-re-head and head-re-body and SC activity is modulated by eye-re-head position. These considerations led us to investigate whether SC activity is modulated by the head-re-body position. We recorded activity from movement-related SC neurons while head-restrained monkeys performed a delayed-saccade task. Across blocks of trials, the horizontal position of the body was rotated under a space-fixed head to three to five different positions spanning ±25°. We observed a significant influence of body-under-head position on SC activity in 50/60 neurons. This influence was expressed predominantly as a linear gain field, scaling task-related SC activity without changing the location of the response field (linear gain fields explained ≥20% of the variance in neural activity in ~50% of our sample). Smaller nonlinear modulations were also observed in roughly 30% of our sample. SC activity was equally likely to increase or decrease as the body was rotated to the side of neuronal recording and we found no systematic relationship between the directionality or magnitude of the linear gain field with recording location in the SC. We conclude that a signal conveying head-re-body position is present in the SC. Although the functional significance remains open, our findings are consistent with the SC contributing to a displacement-to-position transformation for oculomotor control.

INTRODUCTION

Many sensorimotor transformations require integration of the position of the head relative to the body. This is because our major external sensing organs (e.g., eyes and ears) are mounted within the head, which itself is mobile with respect to the body. Consider, for example, the sensorimotor transformations underlying coordinated eye–head gaze shifts to a visual target. For such movements, the retinal representation of the target must be transformed into the appropriate patterns of extraocular and neck muscle recruitment. Within the deeper layers of the superior colliculus (SC), an intermediary for visually guided gaze shifts, movement-related activity is believed to represent desired gaze displacement in an oculocentric frame of reference, encoding the desired gaze shift relative to the current line of sight (Freedman and Sparks 1997b; Mays and Sparks 1980). This displacement-related representation necessitates a transformation into the head-centered and body-centered frames of reference underlying movements of the eyes and head, respectively (Klier et al. 2001). Such a transformation must take into account the initial position of the eye relative to the head and the head relative to the body.

There is circumstantial evidence that the SC may be a component of the network performing this displacement-to-position transformation, at least for the eye component of the gaze shift. Van Opstal and colleagues (1995) demonstrated that the oculocentric representation within the SC in the perisaccadic interval is influenced by initial eye-in-head position. More recently, Campos and colleagues (2006) reported a similar influence of eye position on SC activity during periods of stable fixation in natural scanning and conventional oculomotor paradigms. The influence of initial eye position took the form of a *gain field*, which scaled SC activity without changing the location of the response field. Computational models have shown that gain field modulation of neural activity within the SC and elsewhere could underlie transformations between various frames of reference (Andersen and Buneo 2003; Krommenhoek et al. 1996; Salinas and Abbott 2001; Smith and Crawford 2005).

The goal of this study was to determine whether oculocentrically encoded response fields within the SC are modulated by the position of the head relative to the body. Changes in initial head-on-body position influence the coordination of eye–head gaze shifts (McCluskey and Cullen 2007), as well as the spatiotemporal patterns of neck muscle recruitment during kinematically matched head movements (Corneil et al. 2001). A likely source signaling head-on-body position is the plentiful spindle organs found within the deeper neck muscles adjacent to the spinal column (Bakker and Richmond 1982; Cooper and Daniel 1963; Richmond and Abrahams 1975; Richmond et al. 1999). Mechanical vibration of the muscles of the eyes or neck also influences the metrics of many movements, including saccades (e.g., Corneil and Andersen 2004; Roll et al. 1991; Taylor and McCloskey 1991), and head-restraint and changes in head-on-body orientation influence the localization of auditory stimuli (Goossens and Van Opstal 1999; Populin 2006; Tollin et al. 2005). Finally, profound deficits in balance, posture, and guided actions follow disruption of proprioceptive inputs from neck muscles (Biemond and de Jong 1969; Cohen 1961; de Jong et al. 1977). Presumably, the proprioceptive input from the deep intervertebral muscles provides particularly fine-grain information about the length of neck muscles and the relative position of the cervical vertebrae necessary for many sensorimotor transformations (Abrahams 1977).

Address for reprint requests and other correspondence: B. D. Corneil, Centre for Brain and Mind, Robarts Research Institute, London, Ontario, Canada N6A 5K8 (E-mail: bcorneil@uwo.ca).

To address our experimental goal, we recorded SC activity in monkeys performing a delayed saccade task, examining SC activity during visual, delay, and motor periods (Fig. 1*A*). Across blocks of trials, we rotated the horizontal position of the body under a space-restrained head to specifically manipulate head-on-body position independent of vestibular information. Our results demonstrate a pervasive influence of head-on-body position on the oculocentric command during the motor period, which frequently (but not always) could be described as a linear gain field. Thus the movement-related activity emanating from the SC maintains its oculocentric tuning, but is modulated by information related to head-on-body position. Similar trends were observed for SC activity during the visual and delay periods of the task, although the overall magnitude of modulation was lower than that in the motor period.

Portions of this study were previously published in abstract form (Nagy and Corneil 2007).

METHODS

Subjects and physiological procedures

Two male monkeys (*Macaca mulatta*, monkeys *J* and *M*, weighing 5.4 and 6.8 kg, respectively) were used in these experiments. All training, surgical, and experimental procedures were approved by the Animal Use Subcommittee of the University of Western Ontario Council on Animal Care in compliance with the Canadian Council on Animal Care policy on the use of laboratory animals. Each animal's weight was monitored daily and their general health was under the close supervision of the university veterinarians. Each monkey underwent a surgical procedure to enable single-unit extracellular recordings from the superior colliculus and to enable head restraint and chronic eye position recording. Details of these surgeries have been provided previously (Elsley et al. 2007; Rezvani and Corneil 2008). Briefly, for access to the bilateral SC, a recording chamber (Crist Instruments) was positioned stereotactically over a 19-mm midline craniotomy that allowed a surface-normal approach to the SC (tilted 38° posterior of vertical) and anchored with an acrylic implant. A titanium head bolt for head restraint was also anchored in the acrylic. Preformed eye coils (three turns of stainless steel, Teflon-coated wire, 19–20 mm in diameter; Baird Instruments) were implanted subconjunctivally in both eyes and leads were passed subcutaneously to connectors within the acrylic implant.

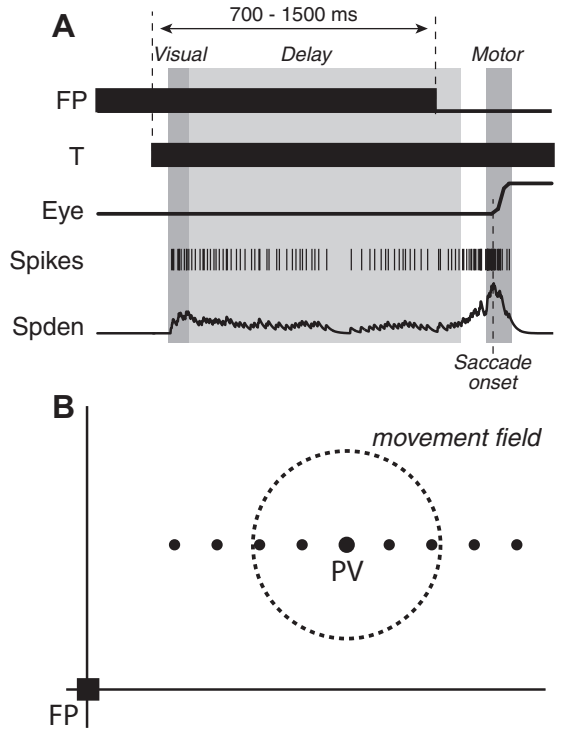

FIG. 1. *A*: the delayed saccade paradigm. Subjects must keep looking at the fixation point (FP) during target (T) presentation and look to the target only after FP disappearance. The interval between T presentation and FP disappearance ranged between 700 and 1,500 ms. Superior colliculus (SC) activity was quantified as a function of head-under-body position during the visual period (50–100 ms after T presentation), the delay period (100 ms after T presentation to 100 ms before the saccade), and the motor period (20 ms before the saccade onset to 8 ms before saccade offset). SC activity is depicted as both a spike rate (Spike) and as a convolved spike density function (Spden); this activity is taken from one trial from the representative neuron shown in Figs. 2–5. *B*: depiction of potential target locations. Over a block of trials, targets were presented symmetrically on a horizontal slice running through the center of the movement field (dashed circle), encompassing the target associated with the neuron's preferred vector (PV).

Experimental procedures

For the duration of each experimental session, the animals were placed in a customized primate chair (Crist Instruments). The chair's design allowed for the interlocking of a head post, eliminating all head movement relative to space. The chair also permitted the computer-controlled rotation of the animal's body under the head. The body was secured within the chair via a back plate and a bar that interweaved between the animal's chest and arms. This configuration restricted active movements of the animal's upper torso to $<5°$. The chair allowed for controlled horizontal rotation of the body under a space-fixed head over a horizontal range of $\pm 40°$, although deviations never exceeded $\pm 25°$ during the recordings reported here. The rotation was performed by a motor at the base of the chair (Shorite Controls, integrated with a chair system by Crist Instruments). This motor rotated the entire chair assembly (including the integrated back plate and interweaving bar, but not the head post) at a peak speed of 3°/s relative to space. This peak speed was sustained for most of the rotation, between periods of gradual acceleration or deceleration that lasted for about 1–2 s. The animals were monitored throughout the experimental session via infrared cameras positioned outside of their line of sight. We also monitored whether the animals were actively resisting body-under-head rotation via a torque sensor attached to the head post and via electromyographic (EMG) electrodes implanted within dorsal neck muscles (Elsley et al. 2007). We found that the animals acclimatized very well to the setup and neither the torque sensor nor the EMG recordings provided any evidence of active resistance to body-under-head rotation.

The experimental sessions were conducted in a dark sound-attenuated room. The animals were placed within the center of a $3 \times 3 \times$ 3-ft gaze-tracking coil system (CNC Engineering) and faced an array of >500 red light-emitting diodes (LEDs) arranged such that they covered $\pm 35°$ of the horizontal and vertical visual fields. These LEDs provided the visual stimuli during the experimental paradigm. LEDs were located along a flat horizontal–vertical rectilinear grid, 1.5 ft from the subjects' head, and were spaced 2° apart from the center of the grid to a horizontal and vertical eccentricity of 20 and 5° apart between 20 and 35° eccentricity. All aspects of the experiment (including the positioning of the chair and monitoring of gaze position) were controlled at a rate of 1 kHz by a National Instruments PXI experimental controller running customized LabVIEW Real-Time programs.

Tungsten microelectrodes (ranging in impedance from 0.5 to 3.0 MΩ at 1 kHz; FHC, Bowdoin, ME) were used to record neural activity. The microelectrodes were lowered via a hydraulic microdrive (Narishige MO-95) through 23-gauge guide tubes held in place by a Delrin grid (Crist Instruments) anchored inside the recording cham-

ber. The guide tubes were designed to end about 2–3 mm above the superficial layers of the SC. Neural activity was amplified, filtered, and stored for off-line sorting via a Plexon MAP system (Dallas, TX). Isolated action potential waveforms that surpassed a user-defined threshold were stored at 40 kHz for off-line spike sorting; the occurrence of extracellular action potentials was recorded at 1 kHz. The majority of our neurons (~75%) were recorded on separate days, with the remainder being recorded simultaneously with another neuron. In the latter case, we ensured via the off-line spike sorter that the recorded waveforms separated into easily isolated clusters.

Behavioral paradigms

Animals were trained to perform a delayed saccade task (Fig. 1*A*), so that the recorded neural activity could be separated into visual-, delay-, and motor-related activity. We specifically searched for SC neurons with movement-related activity. The task began with the presentation of the central LED (the fixation point). The animals were given 1,500 ms to look to the fixation point with an accuracy of ≤3° and maintain central fixation for 750 ms. A peripheral-target LED was then illuminated and the animal had to keep looking at the central fixation point for a pseudorandom period of time, varying between 700 and 1,500 ms (in 100-ms increments). After this delay, the fixation point was extinguished, cueing the animal to make a saccade to the still-visible target. Animals were given 700 ms to look to the target within a radius of 3–5° (less accuracy was required for more peripheral targets) and gaze was to be maintained on the target for 300 ms. If all of the above-cited requirements were met, the animals received a liquid reward and a new trial was initiated. If any of the requirements were violated, the trial was aborted and a pause of 1,000 to 2,000 ms ensued before a new trial was initiated.

Target locations were selected to incorporate the recorded neuron's preferred vector and locations adjacent to this vector. Most of our data were collected with a procedure customized to limit the number of trials required, yet maintain a reasonable amount of statistical power. In this approach, targets were restricted to those spanning a horizontal line through the preferred vector (Fig. 1*B*). The number of targets and the spacing between targets varied from neuron to neuron, depending on the size and center of the movement field (recall the different LED spacing beyond 20°). In most cases, seven or nine targets sufficed to span the movement field. Trials were performed in blocks of 50 to 150 trials per block. Each block was carried out with the monkey's body in one of five positions under a space-fixed head: −25, −12.5, 0, +12.5, and +25° (negative and positive values representing leftward and rightward body-re-head positions, respectively). We defined a complete series of blocks as having a minimum of three body-under-head positions. The first three blocks that we collected were always run with the body at −25, 0, and +25° and the order of body-under-head positions within a given experimental session was randomized across different days. If the quality of isolation permitted further recording, we then ran blocks at −12.5 and +12.5°, again with the order varying across different days. Where conditions would allow, we repeated the five body-under-head blocks a second time. All series contained at least a minimum of 3 blocks with 150 total trials, ≤10 blocks with 1,000 total trials. Over our sample, we were able to obtain an average of 500 to 600 total trials per neuron.

We also collected data from a smaller sample of neurons using a two-dimensional (2D) grid of potential target locations. The potential targets depended on the center and extent of the isolated neuron's movement field and we customized a 5 × 5 array of potential target locations (i.e., 25 potential targets total) to the neuron to ensure a thorough sampling of both the horizontal and vertical extent of the movement field. Within a block of trials for a given head-on-body location, each target location within the central nine locations was sampled more often than the peripheral targets. Because this procedure required substantially more trials per block, we could usually record only two or three different body-under-head locations for a given isolated neuron. This procedure has the advantage of sampling the movement field more extensively, but the disadvantage of obtaining fewer repeated samples for a given target and fewer blocks of trials across different body positions. As will become clear in the RESULTS, we believe the results from this procedure complement the insights obtained from the one-dimensional (1D) procedure, as both procedures have inherent limitations.

Data collection and analysis

Eye movements were first demodulated and then sent to a customized LabVIEW program for paradigm control. Eye movements were sampled at 1 kHz and saved to file. Each trial was manually examined off-line to confirm successful completion. The onsets and offsets of saccades were defined via velocity crossing thresholds of 30°/s. Any trials with anomalous eye movements, excessive delays, or multistep saccades were discarded. Overall, trials were rejected at a rate of <3%.

For off-line analysis, we divided each trial into visual, delay, and motor periods (Fig. 1*A*). The visual period was set to incorporate the peak of the visual burst following target presentation, if present, and spanned from 50 to 100 ms following target onset (Munoz and Wurtz 1995; Sparks et al. 2000). The size of the motor period was set to incorporate the peak of perisaccadic activity and spanned from 20 ms prior to movement onset to 8 ms prior to movement offset (Campos et al. 2006; Miyashita and Hikosaka 1996; Van Opstal et al. 1995). The delay period spanned from 100 ms following target onset to 100 ms prior to movement onset.

Neural activity was quantified using two different methods. First, the number of spikes was counted within each period and then divided by the length of the period, resulting in the average discharge rate over the duration of the period. Second, the spike train was convolved with an excitatory postsynaptic potential (EPSP) function (rise time = 1 ms; decay time = 20 ms), to provide a spike density function that approximates the postsynaptic consequences of neural activity (Thompson et al. 1996). In this study, we primarily report the visual and motor periods via peak discharge rates extracted from the spike density function, although we confirmed that equivalent results were obtained with the average discharge rates. Because the duration of the delay period ranged from 700 to 1,500 ms, we analyzed delay-period activity with average discharge rates.

Response field analysis

The response fields of SC neurons are typically Gaussian in shape, but can be highly asymmetric across stimulus or saccade magnitude. When considering movement fields, for example (i.e., response fields during the movement period), neural activity declines more sharply for saccades that are smaller than the preferred vector (Sparks et al. 1976). Previous studies have also suggested that SC neurons can be characterized as having either "open" or "closed" movement fields (Munoz and Wurtz 1995). Neurons with open movement fields display an elevated and stable level of activity associated with saccades larger than the preferred vector, whereas the saccade-related activity of neurons with closed movement fields declines to zero for saccades larger than the preferred vector.

To accommodate response fields obtained from the 1D sampling procedure with such spatially diverse discharge characteristics, we quantified the response fields by fitting a linearly asymmetric Gaussian to the data. This function is nearly identical to a standard Gaussian, but has one additional term (A) that allows for linear variations in symmetry

$$y(x) = P \exp\left\{ -\frac{(x - C + A|x - C|)^2}{2[W(1 - A^2)]^2} \right\}$$

The A term in the numerator expands or compresses the function along the x-axis, whereas the A term in the denominator serves to

maintain a constant width for varying values of *A*. Unlike the log-Gaussian curve that is sometimes used for movement field analysis (Edelman and Goldberg 2001), this function allows for the capturing of curves with greatly varying levels of symmetry, ranging from perfectly symmetric to completely open. We fit our 2D data with a standard 2D symmetrical Gaussian.

RESULTS

Summary of neuronal sample

We recorded a total of 60 saccade-related neurons in the two monkeys (29 from monkey *M*, 31 from monkey *J*) using the 1D sampling of response fields. The majority of our data analyses will focus on this sample. All 60 neurons displayed a vigorous perisaccadic burst of activity in the motor period, 28 neurons displayed persistent levels of activity during the delay period, and 26 neurons discharged a transient visual burst of activity following target onset. The activity of 28/60 neurons (47%) neurons was examined across three body-under-head positions (center and ±25°; see METHODS), 6/60 neurons (10%) with four body-under-head positions, and 26/60 neurons (43%) with five body-under-head positions. The preferred vectors for the motor-related activity ranged in magnitude from 2 to 37° (mean ± SD: 13 ± 7°) and in radial direction from −63° (i.e., angled below the horizontal axis) to 90° upward (+22 ± 34°). These 60 neurons were found at depths ranging from 450 to 2,450 μm (1,201 ± 523 μm) below the surface of the SC. In the text that follows, we will use the motor-related activity from a representative neuron to illustrate how we fit response fields. We will then examine how the parameters of this fit changed with different body-under-head positions. Finally, we will summarize the results from this analysis across all neurons in our sample for all periods.

Although the horizontal sampling procedure enables a thorough 1D characterization of response fields across different body-under-head positions, this procedure cannot assess the 2D stability of response fields across different body-under-head positions. Accordingly, at the end of RESULTS, we will briefly describe the results of a 2D sampling procedure, which was run on a limited sample of 7 neurons obtained from monkey *M*. Although no neurons were recorded using both the 1D and 2D sampling procedures, this smaller sample of 7 neurons was similar to the larger sample of 60 neurons in all aspects (e.g., all 7 neurons displayed motor-related activity, 3 also displayed visual-related activity, one displayed delay-period activity).

Response field fitting and estimation of variability

Figure 2 shows the activity of a representative neuron for targets placed in the center of the neuron's response field (14° to the right in this example), segregated for three different body-under-head positions (body center, and 25° to the left or right). For all body-under-head positions, this neuron discharged a brief, relatively small burst of action potentials shortly after visual target presentation, continued to emit a persistent level of activity during the delay period, and then emitted a fairly vigorous (~300–400 Hz) burst of action potentials around the time of saccade onset.

Different static body-under-head positions exerted an influence on the movement-related activity of this neuron. This influence is most apparent in the convolved spike-density function, with the magnitude of the movement-related activity during the motor period increasing progressively as the body rotated from right to left. The overall difference in the peaks of the movement-related activity between the far left and far right body positions approached 50 Hz. Although this neuron did display activity during the visual and delay periods, such activity was not consistently modulated by body-under-head position.

Note as well that this neuron displayed activity only during the task. Thus any influence of body-under-head position became apparent only when the monkey was performing the task. This is an observation that was highly consistent across our neuronal sample: we never observed any example of body-under-head position influencing tonic SC activity in task-related neurons during the intertrial interval or during the

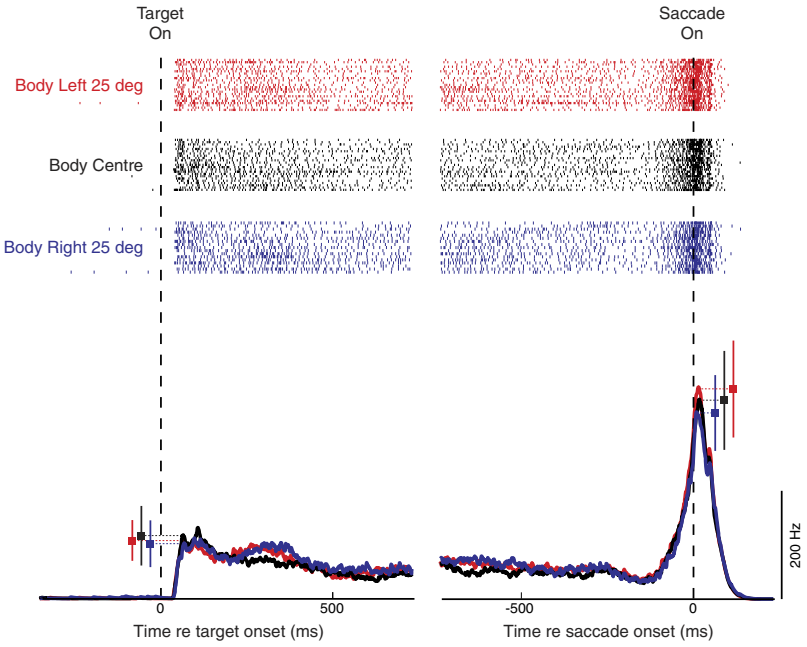

FIG. 2. Activity of a representative SC visuomotor neuron recorded from the left SC, segregated by whether the body was positioned 25° to the left (red lines and symbols), center (black lines and symbols), or 25° to the right (blue lines and symbols) under a space-restrained head. Activity is shown for trials in which the target was presented either at the location associated with the neuron's preferred vector or at either location just beside this location (i.e., 3 locations, with equal sampling of locations across the different body-under-head positions). Neural activity is represented both in a raster format (*top portion*; each tick represents the occurrence of an action potential, with rows of ticks representing different trials) and as a mean convolved postsynaptic activation function (*bottom portion*). Data are aligned to either the time of target presentation (*left portion*) or the time of saccade onset (*right portion*). The squares and vertical lines adjacent to the activation functions represent the mean and SE recorded at time of peak activity either following target presentation (*left portion*) or around saccade onset (*right portion*). Note how the peak of the movement-related activity in particular is influenced by the body-under-head position.

period of stable central fixation prior to target presentation. (Recall we specifically searched for neurons with task-related activity. Accordingly we rarely observed any activity during the intertrial interval or prior to visual target presentation.) This is important since the body-under-head position remained static for ≥50 trials; thus the influences of body-under-head position in these cells emerge only in combination with task-related activity.

Recall that targets were presented at multiple locations spanning a horizontal slice through the response field of the recorded neuron. In Fig. 3, we show the movement field for the same representative neuron when the body was positioned centrally under the head. Although there is some variability, this neuron discharged most vigorously for saccades about 14° in magnitude, with the level of activity falling off for either larger or smaller saccades (i.e., this neuron had a closed movement field). The solid line in Fig. 3 is the fit of the linear asymmetric Gaussian function (see METHODS), permitting quantification of the peak discharge rate (444 Hz) and the center (14.1°), width (5.9°), and symmetry (0.06) of the movement field.

It is important to emphasize that our fitting function provides only single values for the characterization of the response field and thus does not provide any statistical information regarding the variability of these parameters. We therefore performed a bootstrap procedure to iteratively fit multiple curves to this data set. This entailed randomly selecting data points from the existing set, with replacement, to create a new data subset with the same number of data points. A curve was then fit to this new subset and the parameters were extracted. This procedure was repeated 200 times, resulting in 200 estimates for the movement field's peak, center, width, and symmetry. We then used these estimates to derive the variability present in the original data set. Such quantification of variability permits statistical comparisons of response field parameters across various body-under-head positions.

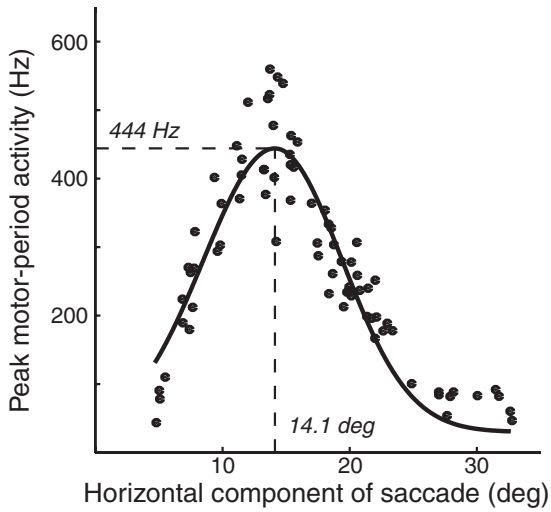

FIG. 3. Movement field of representative neuron shown in Fig. 2, with the body positioned centrally under the head. Each circle represents the peak value of the convolved spike density function from the motor period of a single trial, plotted as a function of the horizontal component of the saccade. The solid line is the linearly asymmetric Gaussian function fit through these data. The center of the movement field for this neuron was about 14°, associated with a peak discharge rate of 444 Hz.

A representative example of how changes in body-under-head position influence movement field parameters

Figure 4 shows a series of movement fields from the representative neuron for five different body-under-head positions. For this example (which is the same representative neuron as shown in Figs. 2 and 3), the center and the general shape of the movement field remained stable as the body rotated though a total of 50° under a space-fixed head. The peak discharge rate at the center of the movement field, however, does decline as the body is rotated from 25° left to 25° right (the peak discharge rate is shown in each subplot in Fig. 4).

The decline in peak firing rate as the body rotates to the right under a space-fixed head is further represented in Fig. 5 for this representative neuron, with each tick representing the peak firing rate extracted from a different iteration of the bootstrap analysis, segregated across the five different body-under-head positions. An ANOVA of peak firing rate across body-under-head position confirmed the significance of the influence of body-under-head position on peak firing rate and a subsequent linear trend analysis (LTA; Keppel and Wickens 2004) confirmed that a significant component of this influence was linear (both $P < 10^{-5}$).

To quantify this influence, we analyzed the data with a linear regression (solid line in Fig. 5) to estimate the change in peak discharge rate as a function of body-under-head position (i.e., the slope of the linear regression line) and to estimate how much of the variability in the data could be accounted for by such changes in body-under-head position (i.e., the r^2 value). For our representative data, the slope of the linear regression line was −1.1 Hz/deg of body-under-head rotation (with the negative sign denoting that the peak firing rate decreased as the body was rotated toward the side of the preferred vector). This slope, which represents the magnitude of a linear gain field, translates into a decrease in peak activity of about 55 Hz over 50° of body rotation or a change of 12.4%. The linear regression demonstrated that 34% of the variability in peak firing rate can be accounted for by the linear change in body-under-head position.

We repeated the preceding analyses on the other parameters of the movement field for the representative neuron (see Table 1 for more detailed results). This analysis revealed a significant but very small change in the center of the movement field. The slope of the linear regression expressing the change in the center of the movement field across different body-under-head rotations was 0.009 Hz/deg of body-under-head rotation, resulting in a change in the center of the movement field of <0.5° across the 50° change in body-under-head position. This result demonstrates that the representative neuron maintained an oculocentric frame of reference during the motor period.

An analogous analysis of the width parameter demonstrated a change of 0.016°/deg body-under-head rotation, equating to a change in the width of the movement field of 0.8° (13%) across the 50° change in body-under-head rotation. However, <0.1% of the variation in the width parameter can be accounted for by linear effects related to changes in body-under-head position. Further consideration regarding the relevance of changes in this width parameter is found in our subsequent summary of the results across our sample.

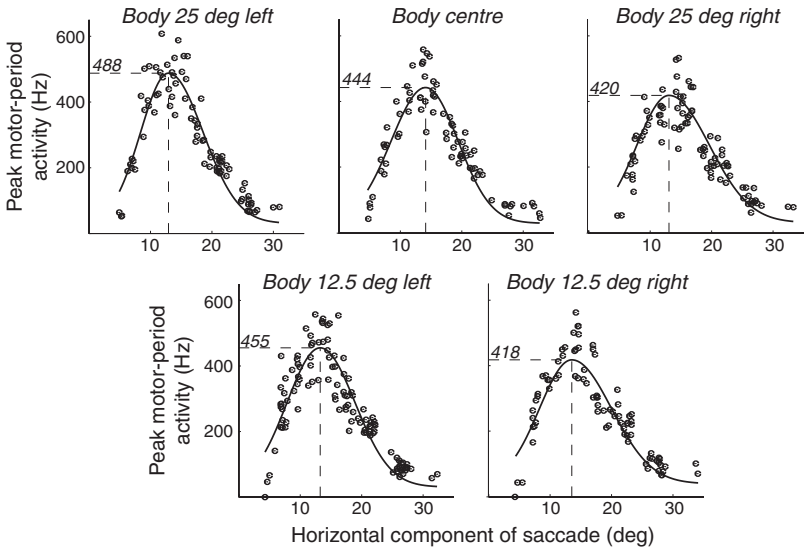

FIG. 4. Movement fields of the same representative neuron shown in Figs. 2 and 3 across 5 body-under-head positions, ranging from 25° left (*top left subplot*) to 25° right (*top right subplot*). Each subplot plots peak motor-period activity vs. horizontal component of saccade, as in Fig. 3. Note that the main change across body-under-head position is in the peak of the movement field (provided in each subplot); there is no obvious systematic change in the center, width, symmetry, or type (i.e., open- vs. closed-movement field) of the movement field in this example.

Analysis of the symmetry variable is more complex, since this is a unitless value that is, arguably, an abstract representation of the shape of the movement field. However, the importance of this parameter should be noted because significant changes in its value may signal a transition from a closed to an open movement field. In the case of the representative neuron, no statistically significant linear trend was found ($P = 0.17$) and all movement fields in Fig. 4 remained closed across all body-under-head positions.

The preceding analyses have focused on the linear component of the modulation in response field parameters with body-under-head position. It is possible that the body-under-head position may solely or additionally modulate response field parameters in a nonlinear fashion. If so, the slope and r^2 values from the regression analysis merely represent the linear component of such a modulation. However, as shown in the following text, whereas nonlinear influences were seen in 19/60 neurons, in most cases the nonlinear component was smaller (in terms of variance explained) than the linear component.

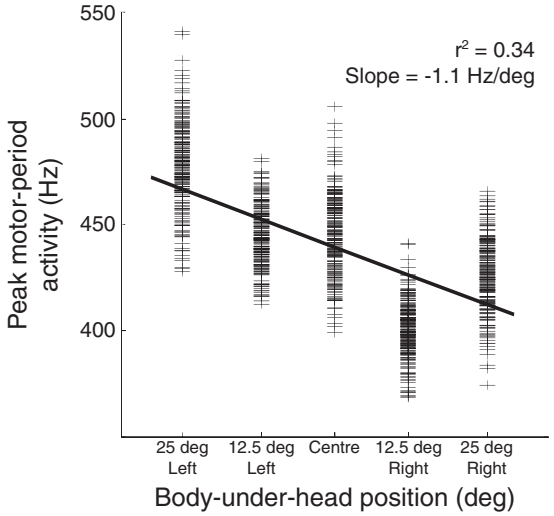

FIG. 5. Results of the bootstrap analysis from the representative neuron shown in Figs. 2–4, with each tick representing the peak value of the movement field for each of the 200 iterations of the bootstrap run at each of the 5 body-under-head positions (see text for more details). Solid line is the linear regression through these data (r^2 and slope value of this regression given in plot, $P < 10^{-5}$). Approximately 35% of the variance in the data is accounted for by the linear trend.

Summary of changes in peak discharge rates across the sample during motor period

We repeated the preceding analyses for all neurons and for all periods in which a given neuron was active (i.e., depending on whether the neuron displayed visual-, delay-, or motor-related activity). We focus first on changes in peak discharge rates in the motor period because this parameter was the most consistently influenced by changes in body-under-head position. For this analysis, we normalized the slopes of the linear regressions for laterality, defining slopes as positive if they increased as the body was rotated toward the side of the preferred vector. Recall our representative neuron (with a preferred vector of 14° right) had a negative slope value, since we observed a decrease in the peak discharge rate as the body-under-head rotated from left to right.

We observed a widespread influence of body-under-head position during the motor period (Table 2). An ANOVA on the peak discharge rates of the 60 neurons in our sample revealed a significant ($P < 0.01$) influence of body-under-head position in 56 (93%) neurons. An LTA performed on these 56 neurons yielded significant ($P < 0.01$) results for 52 neurons and, of these, a linear regression yielded significant ($P < 0.01$) results in 50 neurons. Thus across our sample, the changes in body-under-head position influenced the peak firing rate of 50/60 (83%) neurons in a linear fashion; equivalently, these neurons displayed a linear gain field modulated by body-under-head position.

The linear regression permits quantification of the size and magnitude of the linear gain field via the extracted slope, as well as the amount of variance in peak discharge rate that can be accounted for by body-under-head position. The average magnitude (i.e., the absolute value of the slope) of the linear gain fields was 0.89 ± 0.39 Hz/deg of body-under-head rotation. This equates to a change of about 45 Hz across 50° of body-under-head rotation. In terms of percentages, this amounts to a 0.48% change/deg of rotation or roughly 24% over the 50° range in body-under-head rotation. Of the 50 significant linear regressions, 33, 27, 20, and 14 neurons had an r^2 value >0.1, 0.2, 0.3, and 0.4, respectively.

TABLE 1. *Summary of the statistical analyses of the changes in the movement field parameters across body-under-head position, for the representative neuron*

Parameter	Peak	Center	Width	Symmetry
ANOVA	$P < 10^{-5}$	$P < 0.01$	$P < 0.01$	$P < 0.01$
LTA	$P < 10^{-5}$	$P < 0.01$	$P < 0.01$	$P = 0.094$
Linear regression	$P < 10^{-5}$	$P < 0.01$	$P < 0.01$	$P = 0.17$
Slope	−1.10 Hz/deg	0.0087°/deg	0.0087°/deg	—
Change over 50°	−54.9 Hz	0.433°	0.817°	—
% Change over 50° (relative to value at 0°)	12.4%	3.84%	13.4%	—
Regression r^2 value	0.343	0.0328	<0.001	—

For this table and Table 2, a linear trend analysis (LTA) was run only if the ANOVA was significant and a linear regression was run only if the LTA was significant. Results from the linear regression are presented only if the linear regression was significant. For this representative neuron, the main influence of changes in body-under-head position was on the peak firing rate.

We repeated all of these analyses with an alternative spike-counting methodology that avoids the assumptions inherent to convolving the spike train with an EPSP function. In this methodology, we simply counted the number of spikes within a given interval. With this methodology, the average magnitude (i.e., the absolute value of the slope) of the linear gain fields was 0.86 ± 0.35 Hz/deg of body-under-head rotation. This equates to a change of about 43 Hz across 50° of body-under-head rotation. In terms of percentages, this amounts to a 0.46% change/deg of rotation or about 23% over the 50° range in body-under-head rotation. Of the 50 significant linear regressions, 31, 26, 19, and 13 neurons had an r^2 value >0.1, 0.2, 0.3, and 0.4, respectively. Although these numbers are slightly lower than those observed with the EPSP convolution methodology, the major trends remained. We speculate that the differences between methodologies arise primarily as a consequence of the influence of spikes outside of the relevant intervals (i.e., in the convolution methodology, spikes arriving just before a window influence the spike density function within the window).

Table 3 provides a neuron-by-neuron description of the influence of body-under-head position, with results derived using both the EPSP convolution methodology and the spike-counting methodology.

TABLE 2. *Summary of the patterns of modulation in SC activity due to changes in body-under-head position across the recorded sample*

Pattern	Visual	Delay	Motor
Neurons with observed activity	26	28	60
Significant ANOVA	26	26	56
Significant LTA and linear regression	21	19	50
Unsigned slope magnitude, Hz/deg	0.850	0.347	0.893
Unsigned slope magnitude, %/deg	0.552	1.250	0.476
Average change over 50°, Hz	42.5	17.4	44.6
Average change over 50°, %	27.6	62.5	23.7
Number of neurons with			
r^2 values >0.1	5	7	33
r^2 values >0.2	2	1	27
r^2 values >0.3	1	1	20
r^2 values >0.4	0	0	14

The observed patterns are segregated into the modulation observed in the visual, delay, and motor periods. For each period, *1*) we summarize the number of neurons with a linear gain field (i.e., those in which the LTA analysis yielded a significant result), *2*) the slope of this gain field (expressed in both Hz/deg rotation and percentage change/deg rotation relative to activity with the body at center), and *3*) the amount of variance in activity that could be explained by this activity.

Lack of systematic relationship between horizontal gain fields and movement field parameters

We investigated whether there was any systematic relationship between the slope of the linear gain field both in relation to the direction and magnitude of the preferred vector (since the SC is topographically organized, the magnitude and direction of the preferred vector relate to the neuron's location along the rostrocaudal and mediolateral axes of the SC, respectively). Somewhat surprisingly, we observed no consistent relationships among any of these variables. As shown by the histogram in Fig. 6*A*, the slopes of the fields distributed equally around zero, meaning that the peak discharge rate of a given neuron appeared equally likely to rise or fall as body-under-head position was rotated in the direction of the preferred vector (*t*-test vs. 0, $P = 0.22$). Averaging all of the gain field slopes from Fig. 6*A* yields a sample average of 0.14 ± 0.28 Hz/deg, with 25 neurons favoring body-under-head rotations toward the preferred vector and 25 neurons favoring rotations in the opposite direction. Thus we observed no evidence favoring one direction of body-under-head rotation in our sample.

We observed no relationship between the slope of the linear gain field and the magnitude of the preferred vector, regardless of whether we plotted either the signed (Fig. 6*B*) or absolute magnitudes (Fig. 6*C*) of the slopes as a function of the horizontal component of the preferred vector (qualitatively similar results were obtained by plotting either signed or unsigned gain field slopes as a function of the magnitude of the gaze shift). If anything, our data showed a mild trend for steeper gain field slopes in the rostral versus caudal SC, although neither trend reached significance (Fig. 6, *B* and *C*, respectively; linear regression $P = 0.09$ or $P = 0.12$, respectively).

We also looked for any systematic relationship between gain field parameters and vertical parameters of the preferred vector. These analyses also revealed no systematic relationship between the slope of the linear gain field and either the vertical component of the preferred vector (Fig. 7, *A* and *B*) or the radial direction of the preferred direction (Fig. 7*C*; linear regression, $P > 0.4$ in all cases).

In summary, these analyses revealed that there was no systematic distribution of neurons displaying horizontal gain fields throughout the SC. A given neuron was equally likely to favor body rotations toward or away from the side of recording. Neurons with substantial horizontal gain fields could be found both in the rostral SC encoding relatively small movements and in the most medial or lateral aspects of the SC encoding purely vertical movements.

TABLE 3. *Summary of influence of body-under-head position on motor-period activity for all neurons recorded using a one-dimensional distribution of potential target locations*

				EPSP Convolution			Spike Counting		
Cell	MF	# Pos	Activity	|m|, Hz/deg	Δ50°, Hz	r^2	|m|, Hz/deg	Δ50°, Hz	r^2
je070322_1	10, −4	3	VDM	0.08	4.17	0.07	0.08	4.17	0.07
je070327_2	14, −2	5	VDM	1.77	88.55	0.45	1.71	85.94	0.45
je070322_1	10, −4	3	VDM	0.08	4.17	0.07	0.08	4.17	0.07
je070327_2	14, −2	5	VDM	1.77	88.55	0.45	1.71	85.94	0.45
je070328_1	12, 0	3	VM						
je070328_2	**14, −2**	**5**	**VDM**	**1.10**	**54.90**	**0.34**	**1.09**	**54.56**	**0.34**
je070329_2	14, 2	3	VDM	0.21	10.58	0.02	0.20	10.18	0.02
je070329_3	8, −2	5	VDM	1.27	63.82	0.01	1.23	61.68	0.01
je070329_3	10, −2	5	VDM	0.15	7.82	0.05	0.15	7.61	0.05
je070403_8	4, 4	3	VM	0.42	21.33	0.01	0.40	20.15	0.01
je070411_3	8, −4	5	VDM	0.25	12.53	0.11	0.24	12.06	0.09
je070419_2	6, 0	3	M						
je070424_3a	6, 4	3	M	0.67	33.58	0.48	0.62	31.49	0.48
je070424_3b	6, 2	3	M	0.33	16.67	0.28	0.33	16.66	0.24
je070425_2	2, −4	5	M	0.08	3.97	0.02	0.07	3.71	0.01
je070427_1	4, 0	3	VDM	0.87	43.70	0.53	0.82	41.41	0.46
je070501_2	10, −4	5	M	0.28	14.49	0.25	0.27	13.52	0.23
je070510_1	18, 18	3	M	3.30	165.02	0.89	3.31	165.61	0.74
je070511_1	10, 0	3	VM						
je070514_1a	16, 8	5	VDM	1.42	71.30	0.46	1.30	65.28	0.40
je070514_1b	16, 6	5	M	0.62	31.16	0.03	0.62	31.02	0.03
je070522_2	0, 18	3	M	2.72	136.27	0.78	2.76	138.37	0.64
je070530_2a	6, 16	4	M	0.42	21.44	0.02	0.42	21.25	0.02
je070530_2b	0, 16	4	M	0.40	20.12	0.64	0.39	19.60	0.59
je070531_1	8, 14	3	VDM	0.84	42.49	0.73	0.80	40.06	0.63
je070606_1a	10, −10	4	DM	0.24	12.01	0.05	0.22	11.37	0.05
je070606_1b	8, −10	4	M						
je070608_1	8, −8	5	DM						
je070611_1	10, −8	4	M						
je070612_1	18, 12	4	VDM	2.55	127.65	0.64	2.54	127.06	0.61
je070614_1	18, 20	5	M						
je070620_1	20, 20	3	M	0.58	29.32	0.57	0.56	28.10	0.54
je070627_2	30, 18	5	M	0.28	11.75	0.05	0.22	11.12	0.05
mk070122_4	12, 0	3	VDM	0.69	34.78	0.27	0.68	34.05	0.27
mk070124_1	10, −2	3	DM	0.74	37.14	0.27	0.67	33.90	0.27
mk070125_1	10, −2	3	M	0.65	32.94	0.40	0.60	30.32	0.40
mk070126_1	12, −6	5	M	3.55	177.67	0.36	3.67	183.62	0.31
mk070206_3	6, 16	5	M	2.00	100.05	0.26	1.93	96.82	0.27
mk070207_4	12, 6	5	M	0.28	14.43	0.18	0.30	15.19	0.18
mk070209_1	6, 14	5	VM	0.7521	37.60	0.23	0.72	36.18	0.19
mk070215_4	30, −4	5	VDM	1.3340	66.70	0.25	1.30	65.06	0.22
mk070221_7	4, 10	3	VDM	0.24	12.01	0.11	0.24	12.00	0.09
mk070221_8	6, 12	5	M	1.67	83.95	0.52	1.61	80.95	0.49
mk070222_3a	10, 10	5	DM						
mk070222_3b	18, 10	5	DM	0.98	49.16	0.34	0.99	49.90	0.35
mk070223_3a	6, 8	5	VDM	0.22	11.32	0.01	0.21	10.67	0.01
mk070223_3b	8, 8	5	VDM	0.80	40.19	0.35	0.80	40.00	0.31
mk070223_4a	8, 10	5	M	0.58	29.38	0.01	0.56	28.02	0.01
mk070223_4b	10, 10	5	DM						
mk070223_6	8, 12	3	VDM	0.13	6.72	0.04	0.13	6.70	0.04
mk070228_3	6, 10	3	VDM	2.99	149.50	0.57	2.82	141.10	0.49
mk070302_4a	8, 6	3	M	0.59	29.55	0.32	0.58	29.16	0.29
mk070302_4b	8, 6	3	VDM						
mk070306_5	4, 8	3	VDM	0.79	39.84	0.04	0.74	37.33	0.04
mk070306_7	12, 8	3	M	0.94	47.32	0.31	0.92	46.44	0.30
mk070306_8	14, 8	3	M	0.23	11.50	0.15	0.22	11.14	0.15
mk070307_6	18, 6	3	M	0.27	13.57	0.18	0.25	12.63	0.17
mk070307_8	6, 0	3	VDM	0.52	26.10	0.01	0.50	25.09	0.01
mk070308_2	4, 10	5	M	1.23	61.52	0.02	1.18	59.36	0.02
mk070313_1	8, 0	5	M	0.80	40.30	0.14	0.75	37.72	0.12
mk070313_2	8, 6	3	M	0.47	23.80	0.40	0.43	21.62	0.37
mk070320_2	10, −6	3	VDM	0.04	2.05	0.03	0.03	1.93	0.03
Average				0.89	44.57	0.27	0.87	43.38	0.24

The column "MF" describes the center of the movement field, with the first number representing the contralateral component and the second number representing the vertical component (positive = upward). The column "# Pos" provides the number of body-under-head positions tested. The column "Activity" describes the type of activity displayed by the neuron (V, visual; D, delay; M, motor). Subsequent values provided only for those neurons displaying a statistically significant ANOVA, linear trend analysis, and linear regression. "|m|" denotes unsigned slope value. "Δ50°" denotes change in activity over 50°. All values given for spike density function methodology (columns under "EPSP Convolution") and spike-counting methodology (columns under "Spike Counting"). Data in bold show the representative neuron displayed in Figs. 2–5.

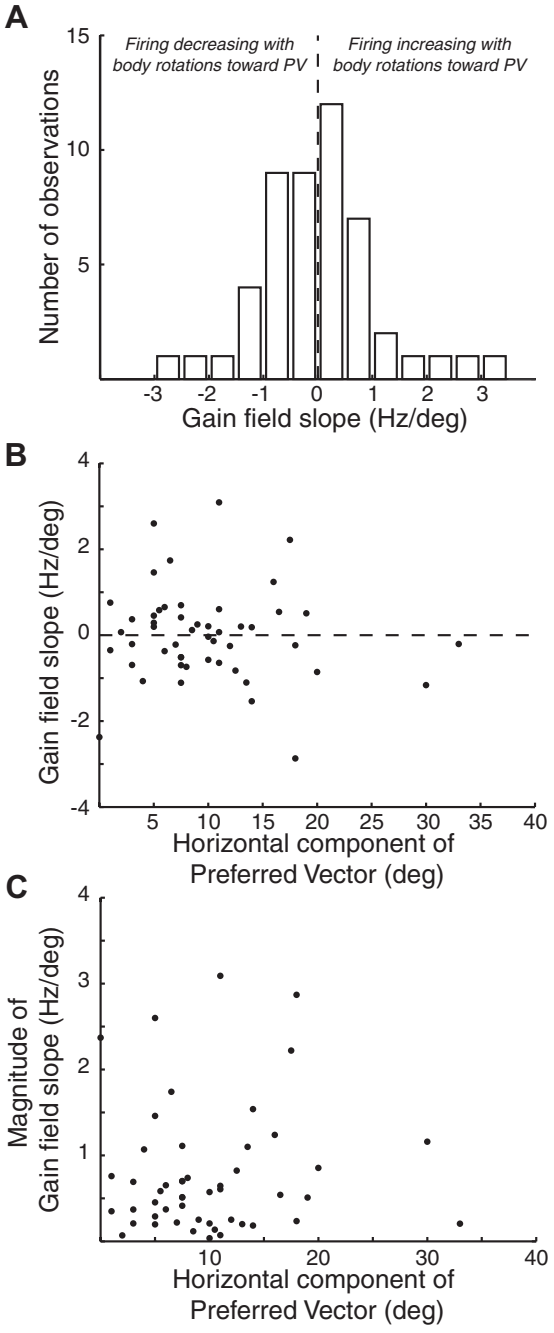

FIG. 6. *A*: histograms of gain field slopes for the subset of 50 neurons displaying a linear gain field modulated by body-under-head position. *B* and *C*: neuron-by-neuron plot of the signed (*B*) or unsigned (*C*) gain field slope as a function of the horizontal component of the preferred vector. Linear correlations on these relationships did not reach significance, indicating that the signed or absolute magnitude of the head-position gain field slope was not significantly influenced by neuron location on the rostrocaudal SC axis.

Summary of changes in peak discharge rates across the sample during visual and delay periods

We repeated the analysis of peak or average discharge rates for those neurons that displayed activity in either the visual period or the delay period, respectively. The results of this analysis are shown in Table 2 and resemble those observed for the motor period. The average unsigned slope of the linear gain field during the visual period was 0.85 ± 0.43 Hz/deg of body-under-head rotation or 0.55%/deg. The r^2 values were considerably lower in the visual period, meaning that less of the variance in peak discharge rate could be accounted by a linear gain field related to head-on-body position. This result may be due to the lower discharge rates for bursts in the visual versus motor period, since any noise that changes the spike rate, even by as few as two to three spikes in the analysis

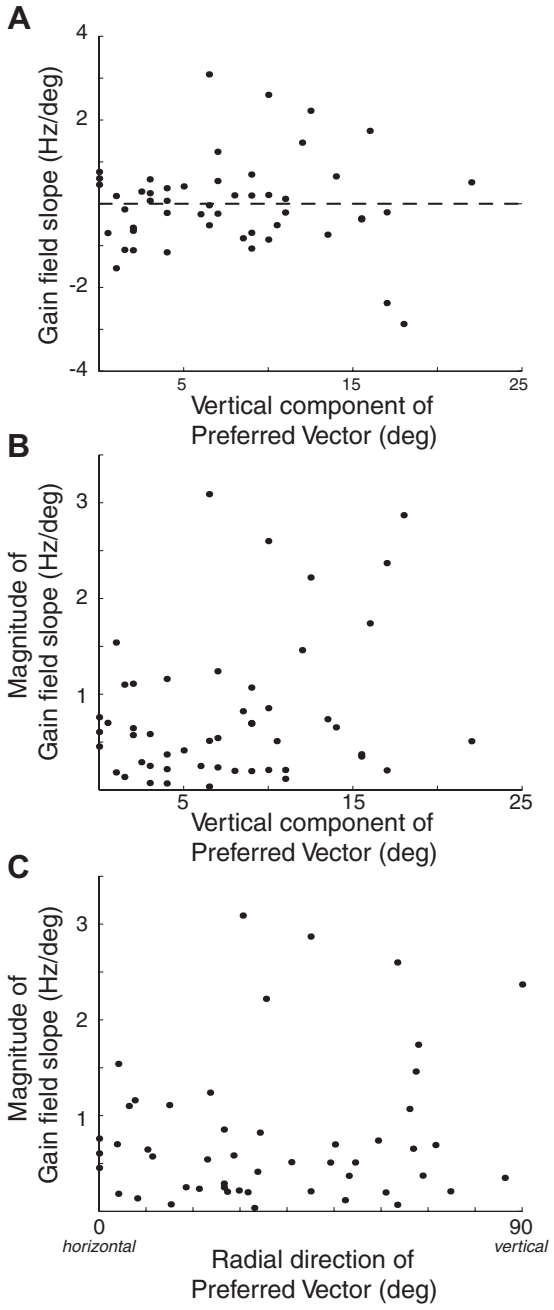

FIG. 7. *A–C*: neuron-by-neuron plot of the signed (*A*) or unsigned (*B*) gain field slope as a function of the vertical component of the preferred vector or of the unsigned gain field slope as a function of the radial direction of the preferred vector (0° denotes purely horizontal movement; 90° denotes purely vertical movements either upward or downward). Linear correlations on these relationships did not reach significance, indicating that larger-magnitude head-position gain field slopes were not confined to those portions of the SC controlling horizontal movements.

window, will have a more pronounced effect in the visual versus motor period.

The results for delay-period activity are slightly different from those for the other periods, mostly because delay-period activity is not a burst, but rather is more persistent throughout the analysis window. The average magnitude of the linear gain field is 0.35 Hz/deg or 1.25%/deg, reflecting the lower discharge rate during the delay period versus the visual and motor periods. The average r^2 values are also lower than those observed during the motor period and resemble the values observed during the visual period.

Finally, we compared the magnitude and direction of the linear gain fields across periods for those neurons that displayed significant gain fields in the motor period and either the visual or the delay period. The results of this analysis are shown in Fig. 8, for a comparison of visual- and motor-period gain fields (Fig. 8*A*) and delay- and motor-period gain fields (Fig. 8*B*). In general, we observed a clear correlation between the signed slopes across these periods, meaning that the sign and magnitude of a gain field in one period related well to the sign and magnitude of a gain field in another period ($r^2 \geq 0.4$ and $P < 0.005$ for both regression lines shown in Fig. 8). Accordingly, there was no systematic distribution of gain fields in the visual and delay periods to favor body rotation in one direction (P of a t-test vs. zero >0.1 for both periods) nor was there any correlation between the signed or absolute magnitudes of gain field slopes versus the magnitude of the preferred vector ($P > 0.1$ for both periods).

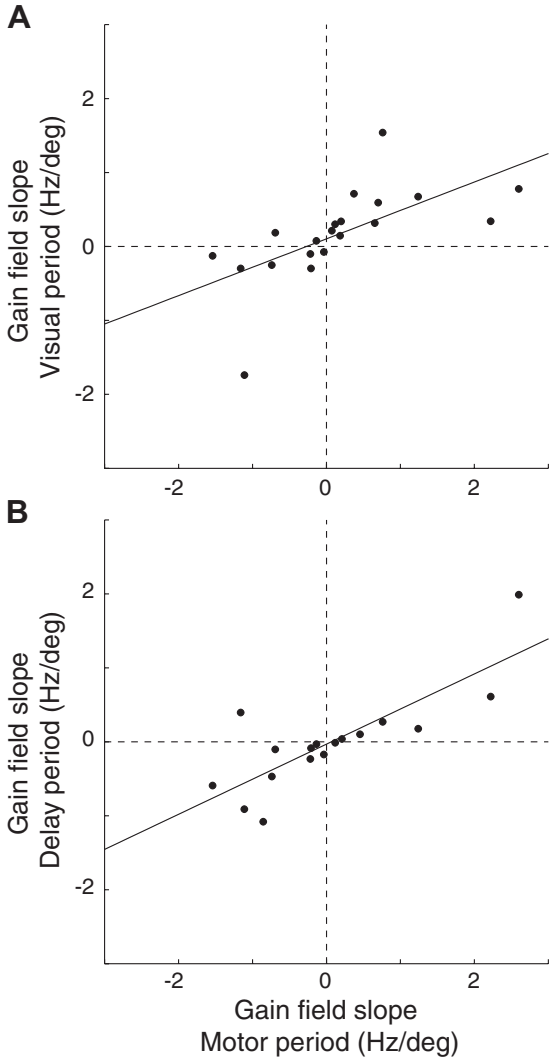

FIG. 8. Comparison of gain field slopes across different intervals, for those neurons displaying gain fields during both the visual and motor periods (*A*) or delay and motor periods (*B*). In both, each square represents data from an individual neuron. Note how points tend to cluster in the *top right* and *bottom left* quadrants, meaning that the signs of gain field tended to remain the same across different intervals. Solid lines show the linear regressions through these data (for *A*, $r^2 = 0.40$, $P = 0.003$; for *B*, $r^2 = 0.65$, $P = 0.0001$).

Summary of changes in other response field parameters across the sample

We repeated this analysis for the other parameters (e.g., response field center, width, or symmetry) fit to the response field for all neurons with activity in the visual-, delay-, or motor-related periods. We excluded five neurons from this analysis since they had incomplete response fields (thus estimates of response field center, width, or symmetry were unreliable). An additional six neurons with open fields had only a partial analysis performed on them, excluding estimates of movement field width or symmetry. We will only briefly summarize the results of this analysis, given that linear modulation of these other parameters tended to be infrequent and small compared with the modulation in peak discharge rate.

We observed no systematic relationship between body-under-head position and the center of the response field in any period. Only 4 of 55 neurons displayed significant linear regressions for changes in the center of the movement field as a function of body-under-head position. Even for these 4 neurons, we observed an average change of $<1°$ in the center of the movement field across 50° of body-under-head rotation. Thus as with the representative neuron, our neuronal sample maintained oculocentric tuning despite changes in body-under-head position.

The general shape of the response field, as defined by the width and symmetry parameters, did show some statistically significant changes across body-under-head position, with 17 neurons showing significant linear trends in at least one of these parameters during the motor period. However, it is important to stress that the majority of these 17 neurons also displayed significant linear changes in peak discharge rate. The most prevalent relationship between these three parameters was that of decreasing width and a tendency toward symmetry for increasing peak discharge rates. Similar to the trends we observed with changes in peak discharge rate, those neurons with significant changes in the width or symmetry parameters were equally likely to favor body-under-head rotation toward or away from the side of recording. Over all our sample, we also never observed any tendency for movement fields to transition from closed to open, or vice versa, across the 50° change in body-under-head position.

Nonlinear modulations in peak discharge rate with changes in body-under-head position

Up to this point, our analysis has focused on describing linear changes in peak discharge rate with body-under-head rotation. This focus on linearity is motivated by our experimental goal to explicitly look for head-position gain fields in the primate SC. Although the modulation of neuronal activity

in most neurons could be described primarily by a linear component, nonlinear modulations were observed in a substantial proportion of neurons. To systematically analyze such nonlinear modulation, we compared the residuals resulting from a linear fit with the residuals from nonlinear fits with polynomials of increasing order up to fourth-order. Second-order polynomials had a single inflection point, whereas third- and fourth-order polynomials had two and three inflection points, respectively. Increasing the order of the fitting function always reduced the residuals, but to deem an increase in order warranted, we arbitrarily decided that an additive increase in r^2 values of $\geq$10% and a significant reduction of residual values as determined by an F-test ($P < 0.01$) were required. The highest order was reached when increases in complexity no longer generated statistically significant reductions in residual values or could not increase r^2 values by 10%. Note that this type of analysis is different from what we performed earlier (where a neuron had to have a significant linear trend to be included in the sample summary). This is because, for example, a neuron characterized with a higher-order fit may or may not have a significant linear component.

Of the 56 neurons that had a significant ANOVA for peak firing rates across body-under-head position, 34 had fits that were best characterized as linear. In other words, a higher-order fit did not provide a statistically significant reduction in residuals and/or did not improve the r^2 values by $\geq$10%. Fifteen neurons, however, showed fits that were characterized as second-order. Only one of these 15 neurons had a negligible linear component and, for the majority of the neurons (11/14), the increase in r^2 value provided by adding the second-order term was less than half the r^2 value of the linear fit (see Fig. 9*A* for an example neuron with a second component). Thus for most neurons characterized as second-order, the linear term was still dominant. Similarly, third- and fourth-order optimal fits were found for 2 and 2 neurons, respectively (see Fig. 9, *B* and *C*, respectively, for examples of neurons with third- and fourth-order components). In total, 53 of the 56 neurons had polynomial fits (linear or otherwise) that significantly reduced the residuals when compared with a fit of constant value and the majority of these were best characterized as linear. However, roughly 30% of our neurons had nonlinear components.

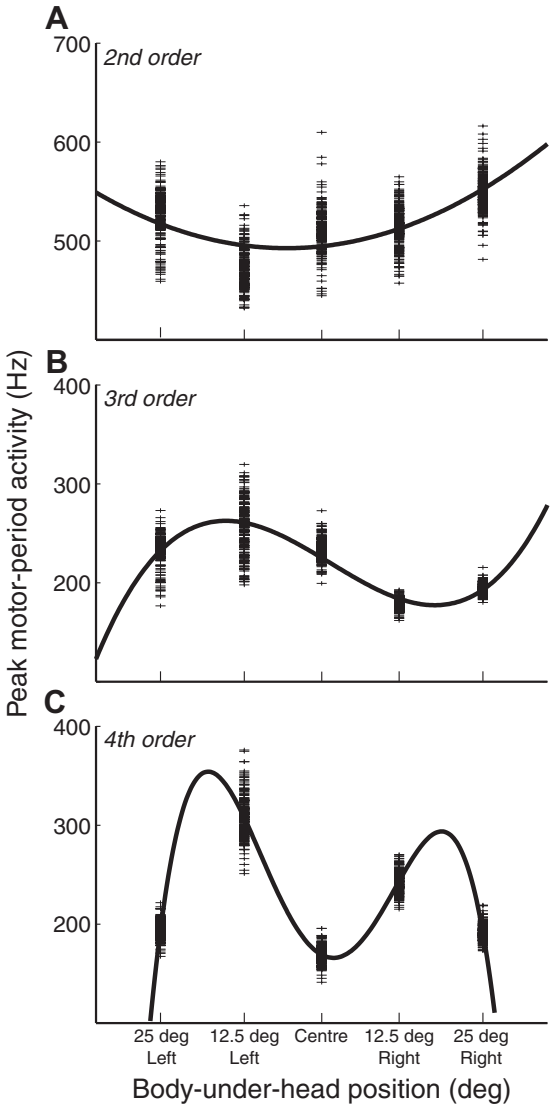

FIG. 9. Examples of neurons with nonlinear modulations of the peak value of the movement field as a function of horizontal body-under-head position (2nd-, 3rd-, and 4th-order fits shown in *A–C*, respectively). Same format as in Fig. 5, with each horizontal tick representing the peak of the movement field derived from one iteration of the bootstrap analysis.

Negligible changes in saccade parameters with body-under-head position

We were interested in whether any aspects of saccade performance varied with body-under-head position because this could provide an alternative explanation for our results (i.e., if saccade velocity changed systematically with body-under-head position, this may explain the observed changes in peak firing rate; see Stanford et al. 1996). To analyze this, we examined whether saccade reaction time, peak velocity, amplitude, and saccade endpoint exhibited any statistically significant changes as body position was rotated under the head. We considered saccades that were made to $\pm$3° around the preferred vector and performed an ANOVA on these values across the three to five body-under-head positions. Out of the 60 sessions from which we collected our neuronal sample, we found significant ($P < 0.01$) changes in reaction time in only 4 sessions, changes in peak saccade velocity in only 3 sessions, and never observed significant changes in either saccade amplitude or endpoint. Thus across our neuronal sample, we are confident that systematic changes in saccade timing or metrics were negligible. Moreover, since the slopes of the gain fields were equally likely to rise or fall as the body was rotated in the direction of the preferred vector, we do not believe that the modulations in SC activity with head-on-body position could be related in any way to changes in saccade parameters.

Stability of neural activity through time

The nature of our experimental protocol required the isolation of SC neurons for a substantial amount of time, both within the block of trials at a given body-under-head position and across all blocks recorded for a given neuron. We were specifically concerned whether there was any evidence that the magnitude of gain fields decreased over time (i.e., as may occur via some sort of adaptation given the prolonged period at a given body-under-head position) or whether ordering of

body-under-head positions sampled for a given neuron influenced the gain field (perhaps because neural activity decreases as the monkeys become satiated). We therefore performed the two following analyses.

First, to address a possible "flattening" of gain fields via adaptation, for a given neuron at each body-under-head position we segregated the neural data into the half collected early within a block of trials and the half collected late in a block of trials. This then allowed us to determine and compare the gain fields for activity collected "early" and "late" within a block of trials, using the bootstrap analysis described earlier. We observed no tendency for gain field slope to change in any way (F-test performed on a neuron-by-neuron basis for all neurons displaying a significant gain field within a given interval; $P > 0.05$ for all neurons, with $P > 0.01$ for all but two neurons within our sample).

Second, to address the possible ordering effects related to the selected body-under-head positions through time, we shuffled our data set so that peak firing rates were assessed based on the rank order at which they were assessed rather than by body-under-head position (e.g., imagine the peak firing rate estimates in Fig. 5 plotted as a function of rank order of blocks, rather than by body-under-head position). We then repeated all of our previous analyses and found significant results in only 2 of our 60 neurons (i.e., in these 2 neurons, an apparent gain field could have arisen simply because of the ordering in which we sampled body-under-head position). This number is far less than our main results; thus we do not believe that ordering effects are a major concern (recall as well that the veridical gain fields we describe were equally likely to rise or fall across different body-under-head positions).

Two-dimensional stability of movement fields across different body-under-head positions

One potential concern about data reported up to now is that the response fields were assessed via a 1D horizontal slice through the neuron's preferred vector. Is it possible that our results could be due, at least in part, to selective changes in the vertical aspects of the response field (e.g., center or shape of the response field) that went undetected? To address this question, we turn now to the sample of seven neurons obtained with a 2D sampling procedure that spanned both the horizontal and vertical extents of the response field.

Figure 10 shows the movement field of one of these seven neurons with the body positioned under the head either 20° left

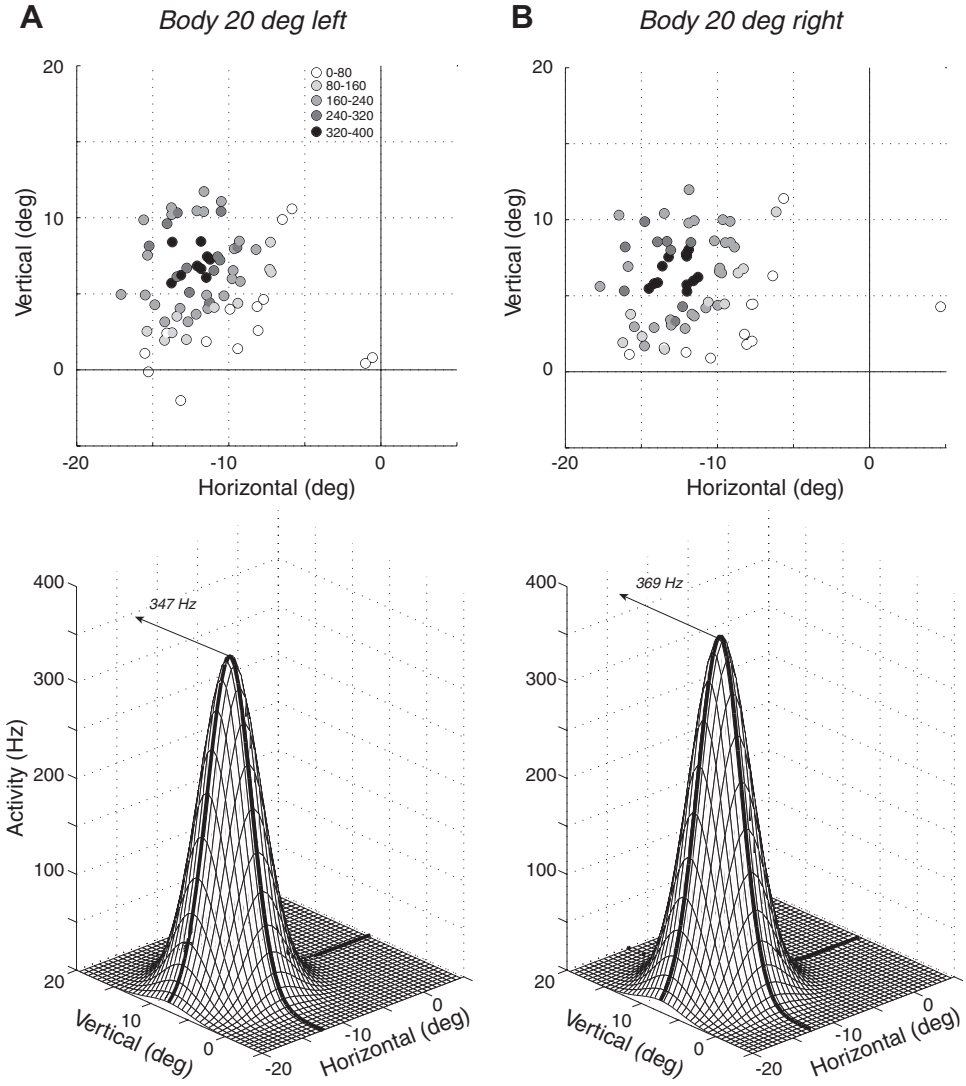

FIG. 10. Representative example of the influence of body-under-head position on a movement field assessed with a 2-dimensional (2D) distribution of potential target locations, with body rotated either 20° left (*A*) or right (*B*). In each subpanel, the *top plot* shows a 2D distribution of saccade endpoints, with the circle shading denoting the peak amount of activity during the movement interval. The *bottom plot* shows the 2D Gaussian fit to these data. Note the change in peak activity of the movement field without a change in the center of the movement field.

(Fig. 10*A*) or 20° right (Fig. 10*B*). The main point of this figure is to demonstrate that although the peak activity of the response field changed with body-under-head position (from 347 Hz in Fig. 10*A* to 369 Hz in Fig. 10*B*), the center of the movement fields appeared stable (12.5° left, 7.5° up in both body-under-head positions). To quantitatively analyze these data, we ran a version of our bootstrap analysis modified for 2D movement fields (using 100 iterations of the bootstrap procedure). In the case of this neuron, the peak activity was the only parameter to change significantly ($P < 0.01$; gain field slope: 0.55 Hz/deg or 0.15%/deg; neither the *x*- nor *y*-position of the movement field center changed significantly, $P = 0.47$ or 0.32, respectively).

We repeated this analysis for the other six neurons. One other neuron displayed a significant gain field, also without displaying any change in the center of the movement field. The remaining five neurons did not display significant gain fields, nor did they display any change in the center of the movement field. In summary, although the collection of seven neurons assessed with the 2D sampling procedure is relatively small, we did not observe any evidence for changes in the center of the response field, nor for selective changes in the vertical but not horizontal position of the response field. As with our sample of data collected with a 1D sampling procedure, the peak of the movement field appeared to be the parameter most susceptible to influence of body-under-head position.

DISCUSSION

Neurons within the primate superior colliculus project to the premotor circuits for eye and head movements and provide the command for saccadic gaze shifts. This command is expressed in oculocentric coordinates, specifying the metrics of the desired gaze shifts relative to the current line of sight (Freedman and Sparks 1997b; Robinson 1972; Sparks and Mays 1983). Here, we demonstrate for the first time that this oculocentric representation is modulated by the horizontal position of the head relative to the body. The predominant form of this modulation is as a linear gain field, with the major effect being a scaling of the level of activity for movements at or near the preferred vector. Similar patterns of modulation were seen in the neural activity following visual target onset and during a delay period interposed between sensation and movement and gain field slopes and magnitudes were well correlated on a neuron-by-neuron basis across all periods. We observed no systematic relationship between the magnitude or directionality of the slope of the gain field with either the side or location of recording within the SC motor map. Taken with reports of modulations of task-related activity in other oculomotor areas with either eye-in-head or head-on-body position, our results provide support for the notion that SC activity is multiplexed with signals representing the body's current configuration. Precisely how this head-on-body position signal is used by downstream targets of the SC—or whether it is even used at all—remains an open question.

Comparison with previous results and methodological concerns

Previous reports have established that variations in initial eye and/or head position modulate oculomotor-related activity throughout the oculomotor system (parietal cortex: Brotchie et al. 1995; Snyder et al. 1998; frontal cortex: Cassanello and Ferrera 2007a; superior colliculus: Campos et al. 2006; Van Opstal et al. 1995). Our results are in good agreement with the results of Van Opstal et al. (1995) and Campos et al. (2006) who investigated modulation of SC activity with initial eye position, despite considerable differences in experimental methodology and the methods for quantifying gain fields (e.g., both the Van Opstal and Campos studies used free-scanning paradigms). By integrating our results with those of Van Opstal and Campos, it becomes apparent that a substantial proportion of SC neurons are modulated by initial eye or head position: eye-position gain fields were reported in 30/57 (53%) of neurons by Van Opstal et al. (1995) during the motor period and in 16/73 (21%) of neurons by Campos et al. (2006) during periods of stable fixation. We observed head-position gain fields with $r^2 > 0.2$ in 27/60 (45%) neurons of our sample during the motor period. The magnitudes of modulation with body-under-head position (i.e., the absolute values of the slopes of the gain fields) that we observed (~1 Hz/deg during the motor period) are notably smaller than the comparable value reported by Van Opstal and colleagues (~3–5 Hz/deg of eye position), but this may be in part due to the restriction of our experimental setup to horizontal body-under-head rotations. Thus we were limited to studying only the horizontal component of any head-position gain field.

One substantial difference between our results and those describing eye-position gain fields in the SC is the lack of colinearity that we observed. Colinearity describes the alignment of the direction of the gain fields with movement field and, although we could assess only the horizontal components of head-position gain fields, neural activity was equally likely to increase or decrease as the body was rotated in the direction of the preferred vector. In contrast, both Van Opstal and colleagues (1995) and Campos and colleagues (2006) reported that gain fields tended to align with the direction of the neuron's movement field.

We find the lack of observed colinearity in our experiment to be puzzling and have no straightforward explanation. The majority of head-position gain fields in the lateral intraparietal area (area LIP) are colinear (Brotchie et al. 1995), making our observed lack of colinearity all the more surprising, given that area LIP is a likely source of the SC head-position gain fields (see next section). However, it is possible that the lack of colinearity in the SC reflects the convergence of head-position gain fields from both the parietal and frontal cortices. Although a systematic study of head-position gain fields in the saccade portion of the frontal eye fields (FEFs) has not yet been undertaken, eye-position gain fields in the FEF are strongly aligned *opposite* to the direction of the movement fields (Cassanello and Ferrera 2007a). A particularly important future experiment will be to compare the directionality of eye and head-position gain fields in the SC in the same neuron. Within area LIP, eye- and head-position gain fields corresponded in both directionality and magnitude, summing into a gain field encoding gaze position relative to the body, regardless of whether the eyes or the head redirects gaze (Brotchie et al. 1995; Snyder et al. 1998). Whether a similar encoding of gaze position relative to the body exists in the SC remains to be determined.

Our findings of horizontal head-position gain fields throughout the rostrocaudal extent of the SC (Fig. 6) demonstrate that

a sensitivity to head-on-body position is not limited to those portions of the SC typically associated with head movements, but that such sensitivity can be found even in relatively rostral locations that encode small gaze magnitudes. Our findings that horizontal head-position gain fields can also be found in the most medial or lateral portions of the SC encoding vertical movements (Fig. 7) demonstrate that such sensitivity is also not simply restricted to the central portion of the SC encoding horizontal movements. This observation can be seen as an extension of the lack of colinearity; we also observed a lack of parallelism, in that horizontal head-position gain fields could be observed even in neurons encoding strongly vertical movements. It therefore appears that the signal representing horizontal head position is distributed throughout the entire saccadic-related portion of the SC.

A novel aspect of our results is the description of nonlinear modulation. Across our sample, the fits of 19 of our neurons were significantly improved by the addition of a nonlinear term. Although nonlinear gain fields were not reported in the SC studies of either Van Opstal and colleagues (1995) or Campos and colleagues (2006), the prevalence of nonlinear components reported here parallels descriptions of eye-position gain fields in parietal areas 7a and LIP (Andersen et al. 1990). Andersen and colleagues (1990) describe that roughly 50% of parietal neurons have linear gain fields ("planar" in their terminology, since eye position was assessed in two dimensions), roughly 40% have gain fields that have a linear component and nearly 10% of neurons have nonlinear gain fields. Previous reports of head-position gain fields in area LIP (Brotchie et al. 1995; Snyder et al. 1998) have not considered the possibility of nonlinear modulations, in part because such studies have typically examined only two horizontal body-under-head positions. The functional relevance of such nonlinear gain fields, if any, remains to be determined, although we note that computational models of reference frame transformations can incorporate gain fields with both linear and nonlinear components (Pouget and Sejnowski 1997). It is important to emphasize, however, that although nonlinear modulations are present in our sample, such components tend to be less prevalent and explain less of the variance than do linear components.

One potential concern about our data set is that most was collected with a 1D horizontally orienting "slice" of potential target locations through the center of the movement field. Theoretically, the gain fields that we have observed could be due to selective vertical shifts in the center of the movement field that went undetected. Our small sample of neural activity with a 2D distribution of potential target locations makes this possibility unlikely, given that we did not observe any evidence for the center of the movement field to shift in any way. Furthermore, the observed lack of colinearity would necessitate idiosyncratic, and selective, shifts in the vertical position of the movement field (recall our gain field slopes were equally likely to favor body rotations toward or away from the side of recording). Thus we believe it is highly unlikely that the data sampled with the 1D methodology could be explained by selective shifts in the vertical position of the movement field.

Finally, it is important to acknowledge a selection bias inherent to our experiment. Because we sought to systematically alter body-under-head position, we restrained the head in space. Such head-restraint precludes the recording of putative head-only neurons reported recently to exist within the SC (Walton et al. 2007), since such neurons are functionally identified by their contribution to head movements without gaze shifts. We also did not explicitly target the rostral SC. Thus our observations are restricted to saccade-related SC neurons.

Possible sources and routes of head-position input to the superior colliculus

Rotating the body under a space-fixed head stretches muscles and ligaments within the neck. We attribute our main experimental result to altered proprioceptive input originating for the many receptors embedded within the soft tissues of the neck (Bakker and Richmond 1982; Richmond and Abrahams 1975). The nature of our paradigm was fundamentally static, in that the body-under-head was positioned to a given location for a subblock of $\geq$50 trials and proprioceptive sources are ideally suited to provide length-dependent information during these static subblocks. We cannot exclude the potential contributions of other sources, such as efference copy or residual inputs from vestibular sources, but it seems rather unlikely that such nonproprioceptive sources play a principal role. Simultaneous recordings of neck muscle activity and head torque provided no evidence that the animals were actively resisting body-under-head rotation and any movement of the head in space was likely very small and limited only to the time of body-under-head rotation. Furthermore, vestibular stimulation does not have a significant influence on the firing of SC neurons (Hepp et al. 1993; Walton et al. 2007).

Assuming that proprioceptors within the soft tissues of the neck are the primary source of head-on-body information, what then are the possible routes by which this information accesses the SC? Subcortical routes are certainly plausible, given the effects of neck muscle stimulation on SC activity in anesthetized cats (Abrahams and Rose 1975; Abrahams and Turner 1981) and the termination of neck muscle afferents in brain stem areas, which themselves project to the primate SC (Edney and Porter 1986). However, neck proprioceptive information is commonly combined with vestibular information at many subcortical centers, including the vestibular nuclei and cerebellum (for review, see Richmond and Corneil 2001), yet the apparent selective sensitivity of SC neurons to proprioceptive stimulation requires segregation of proprioceptive and vestibular information. Furthermore, we surmise that the expression of a linear head-position gain field consequent to body-under-head rotation requires the integration of proprioceptive information across multiple cervical segments, since proprioceptive density is greatest within the deeper muscles of the neck that span individual cervical vertebrae (Richmond and Bakker 1982; Richmond et al. 1999). The integration of proprioceptive information across multiple cervical vertebrae into a linear signal expressing the position of the head relative to the body would seem to require multiple levels of sensory convergence and processing. We therefore view it as likely that at least a portion of the head-position influence on the SC stems from cortical sources.

A very plausible cortical candidate for relaying head-position information to the SC is area LIP. As mentioned earlier, the activity of neurons within area LIP is modulated by body-under-head position (Brotchie et al. 1995) and, impor-

tantly, such modulation is segregated from vestibular information (Snyder et al. 1998). Although area LIP neurons do send functional projections to the SC (Paré and Wurtz 1997, 2001), it remains to be determined whether such projections convey head-position gain fields (although this seems likely considering the evolution of signals from the cortex to SC; see Wurtz et al. 2001). However, our observed lack of colinearity between head-position gain fields and the movement field suggests that area LIP is not the sole source of head-position information. A modulating influence of head-on-body position in the saccade-related region of the primate FEF has never been explicitly tested. However, preliminary reports describe a modulating influence of head-on-body position in the smooth-pursuit–related area of the FEF (Fukushima 2007) and neural activity within the saccade-related area of FEF is gain-modulated by eye-in-head position (Cassanello and Ferrera 2007a). The feline homologue of the FEF also receives afferent information from neck muscles (Barbas and Dubrovsky 1980; Dubrovsky and Barbas 1977), making it possible that the FEF may also provide head-on-body signals to the SC.

Possible functional roles for head-position gain fields in SC

What then is the functional purpose of head-position sensitivity that we have observed within the primate SC? In this section, we consider briefly three alternatives, as well as the implications of such alternatives on current notions of reference frame transformations and SC coding. Our data set cannot differentiate between these three possibilities, but it is important to stress that these considerations must be made in light of the acknowledged influence of initial eye and head position on the elaboration of eye and head movements during gaze shift (Becker and Jurgens 1992; Freedman 2005; Freedman and Sparks 1997a; Goossens and Van Opstal 1997; McCluskey and Cullen 2007; Volle and Guitton 1993). Thus it is not a question of whether influences of body configuration on the programming of gaze shifts exist, but rather whether the neural network(s) that impart such influences incorporate the SC.

The first possibility is that what we are observing is simply an epiphenomenon that reflects the position of the SC within the sensorimotor pathway for saccades, downstream of area LIP. The lack of any colinearity between the parameters of the head-position gain fields (e.g., peak discharge rate, width, or symmetry) and movement fields means that the signal encoding head-on-body position could cancel out in a straightforward fashion in a downstream population coding scheme. For example, the resultant overall spike count (Van Opstal and Goossens 2008) or vector average (Lee et al. 1988) would continue to express the gaze command in oculocentric coordinates across all body-under-head positions. Although plausible, this possibility necessitates that mechanisms that implement the well-known influences of initial eye-in-head and head-on-body position on gaze shift elaboration exist downstream of, or in parallel to, the SC.

A second possibility is that the SC is indeed a component of the network involved in the decomposition of a gaze-related command into the component movements of the eyes and head, providing a multiplexed signal expressing both the desired gaze shift and the aspects of initial body configuration. If true, it will be important to determine whether eye- and head-position gain fields in the SC sum into a gain field expressing gaze position relative to the body, as appears to be the case in area LIP (Brotchie et al. 1995). Theoretically, the appropriate head-referenced and body-referenced commands for the eye-in-head and head-on-body commands, respectively, can be extracted from this multiplexed signal via models that incorporate gain fields (Xing and Andersen 2000; Zipser and Andersen 1988). This can be done regardless of whether the SC neurons express integrated gaze gain fields or independent eye- and head-position gain fields or whether the gain fields are colinear, although the network architectures underlying such transformations will be different (Xing and Andersen 2000) and thus constrained by neurophysiological findings.

An issue related to this second alternative is whether the signal—which we presume has a proprioceptive origin given the static nature of our task—can be updated rapidly enough for the dynamic control of action. Behavioral evidence suggests that the brain is capable of updating target locations in space to ensure accurate eye–head gaze shifts essentially instantaneously, despite intervening or ongoing motion (Corneil et al. 1999; Vliegen et al. 2004, 2005). Evidence from anesthetized cats suggests that the minimal response latencies of tectospinal neurons following electrical stimulation of neck muscle proprioceptors range between 10 and 50 ms (Abrahams and Rose 1975). Such response latencies are likely too slow for on-line control of behavior. If head-position gain fields in the SC do play a functional role in on-line control of behavior, then they would have to be supplemented with other sources, such as efference copy, that do not have inherent delays.

Finally, a third possibility that lies somewhat intermediate between the two other alternatives is that eye- and head-position gain fields in the SC are cancelled out in downstream SC projections, but participate in other functions by virtue of upstream projections through, for example, the thalamus (Sommer and Wurtz 2008). A recent study by Cassanello and Ferrera (2007b) demonstrated that the anticollinear eye-position gain fields in the FEF could theoretically drive visual remapping during saccades; the dynamic integration of stimuli of different sensory modalities with gaze shifts may well require input conveying head-on-body information (Goossens and Van Opstal 1999; Vliegen et al. 2004, 2005). Campos and colleagues (2006) similarly proposed that the eye-position signals within the SC, particularly during fixation intervals, may be relevant for planning sequences of multiple saccades or head-free gaze shifts. This alternative would also necessitate that networks that do not include the SC are responsible for implementing the influences of initial eye and head position on gaze shifts.

A recent report by Wang and colleagues (2007) surmised a calibration role for eye muscle proprioception. We find it difficult to conceive that movement-related SC neurons could fulfill a similar role for the calibration of head-on-body position. The expression of head-on-body information on SC neurons is phasic and would thus be available only in a task-related manner; we never encountered a neuron that tonically expressed head-on-body position. Such a phasic representation differs from the tonic expression of eye-in-head position observed by Wang and colleagues in the primary somatosensory cortex. Our observations do not preclude the possibility that neck muscle proprioception plays a calibration role in other brain areas.

Summary and conclusions

In conclusion, we have reported a marked modulation of SC activity with head-on-body position. The level of modulation averages around 1 Hz per degree change in head-re-body position, even though we were restricted to horizontal rotations of the body under the head. These findings demonstrate additional representations of initial body configuration within the SC and thus have important implications regarding both precisely what is encoded by SC activity and where sensorimotor transformations take place. The importance of the posterior parietal cortex in sensorimotor transformations has long been recognized, given the modulating influences of initial body configuration on response fields (for review, see Andersen and Buneo 2003). Our observations of head-position gain fields in the SC—in addition to previous reports of eye-position gain fields—suggest that similar transformations may be housed within a structure notably closer to the motor periphery.

ACKNOWLEDGMENTS

We thank Dr. Paul Gribble for advice on the bootstrap and nonlinear analyses used in this manuscript and K. Barker and T. Admans for outstanding technical and animal husbandry assistance, respectively.

GRANTS

This work was supported by Canadian Institutes of Health Research (CIHR) Operating Grant MOP 64202 to B. D. Corneil, a Career Development Award from the Human Frontier Science Program to B. D. Corneil, a CIHR Group Grant, and infrastructure support from the Canadian Foundation for Innovation and the Ontario Innovation Trust. B. D. Corneil is a CIHR New Investigator.

REFERENCES

Abrahams VC. The physiology of neck muscles; their role in head movement and maintenance of posture. *Can J Physiol Pharmacol* 55: 332–338, 1977.

Abrahams VC, Rose PK. Projections of extraocular, neck muscle, and retinal afferents to superior colliculus in the cat: their connections to cells of origin of tectospinal tract. *J Neurophysiol* 38: 10–18, 1975.

Abrahams VC, Turner CJ. The nature of afferents from the large dorsal neck muscles that project to the superior colliculus in the cat. *J Physiol* 319: 393–401, 1981.

Andersen RA, Bracewell RM, Barash S, Gnadt JW, Fogassi L. Eye position effects on visual, memory, and saccade-related activity in areas LIP and 7a of macaque. *J Neurosci* 10: 1176–1196, 1990.

Andersen RA, Buneo CA. Sensorimotor integration in posterior parietal cortex. *Adv Neurol* 93: 159–177, 2003.

Bakker DA, Richmond FJ. Muscle spindle complexes in muscles around upper cervical vertebrae in the cat. *J Neurophysiol* 48: 62–74, 1982.

Barbas H, Dubrovsky BO. Characteristics of dorsal neck muscle afferent input to the cat frontal cortex before and after dorsal funiculus section. *Exp Neurol* 67: 35–51, 1980.

Becker W, Jurgens R. Gaze saccades to visual targets: does head movement change the metrics? In: *The Head–Neck Sensory Motor System*, edited by Berthoz A, Graf W, Vidal PP. New York: Oxford Univ. Press, 1992, p. 427–433.

Biemond A, de Jong JM. On cervical nystagmus and related disorders. *Brain* 92: 437–458, 1969.

Brotchie PR, Andersen RA, Snyder LH, Goodman SJ. Head position signals used by parietal neurons to encode locations of visual stimuli. *Nature* 375: 232–235, 1995.

Campos M, Cherian A, Segraves MA. Effects of eye position upon activity of neurons in macaque superior colliculus. *J Neurophysiol* 95: 505–526, 2006.

Cassanello CR, Ferrera VP. Computing vector differences using a gain field-like mechanism in monkey frontal eye field. *J Physiol* 582: 647–664, 2007a.

Cassanello CR, Ferrera VP. Visual remapping by vector subtraction: analysis of multiplicative gain field models. *Neural Comput* 19: 2353–2386, 2007b.

Cohen LA. Role of eye and neck proprioceptive mechanisms in body orientation and motor coordination. *J Neurophysiol* 24: 1–11, 1961.

Cooper S, Daniel PM. Muscle spindles in man; their morphology in the lumbricals and the deep muscles. *Brain* 86: 563–586, 1963.

Corneil BD, Andersen RA. Dorsal neck muscle vibration induces upward shifts in the endpoints of memory-guided saccades in monkeys. *J Neurophysiol* 92: 553–566, 2004.

Corneil BD, Hing CA, Bautista DV, Munoz DP. Human eye–head gaze shifts in a distractor task. I. Truncated gaze shifts. *J Neurophysiol* 82: 1390–1405, 1999.

Corneil BD, Olivier E, Richmond FJ, Loeb GE, Munoz DP. Neck muscles in the rhesus monkey. II. Electromyographic patterns of activation underlying postures and movements. *J Neurophysiol* 86: 1729–1749, 2001.

de Jong PT, de Jong JM, Cohen B, Jongkees LB. Ataxia and nystagmus induced by injection of local anesthetics in the neck. *Ann Neurol* 1: 240–246, 1977.

Dubrovsky BO, Barbas H. Frontal projections of dorsal neck and extraocular muscles. *Exp Neurol* 55: 680–693, 1977.

Edelman JA, Goldberg ME. Dependence of saccade-related activity in the primate superior colliculus on visual target presence. *J Neurophysiol* 86: 676–691, 2001.

Edney DP, Porter JD. Neck muscle afferent projections to the brainstem of the monkey: implications for the neural control of gaze. *J Comp Neurol* 250: 389–398, 1986.

Elsley JK, Nagy B, Cushing SL, Corneil BD. Widespread presaccadic recruitment of neck muscles by stimulation of the primate frontal eye fields. *J Neurophysiol* 98: 1333–1354, 2007.

Freedman EG. Head–eye interactions during vertical gaze shifts made by rhesus monkeys. *Exp Brain Res* 167: 557–570, 2005.

Freedman EG, Sparks DL. Eye–head coordination during head-unrestrained gaze shifts in rhesus monkeys. *J Neurophysiol* 77: 2328–2348, 1997a.

Freedman EG, Sparks DL. Activity of cells in the deeper layers of the superior colliculus of the rhesus monkey: evidence for a gaze displacement command. *J Neurophysiol* 78: 1669–1690, 1997b.

Fukushima K. Vestibular and neck proprioceptive inputs to pursuit neurons in the frontal eye fields (Abstract). *Proceedings of the 17th Annual Meeting of the Society for the Neural Control of Movement, Seville, Spain, March 2007*. NCM, 2007.

Goossens HH, Van Opstal AJ. Human eye–head coordination in two dimensions under different sensorimotor conditions. *Exp Brain Res* 114: 542–560, 1997.

Goossens HH, Van Opstal AJ. Influence of head position on the spatial representation of acoustic targets. *J Neurophysiol* 81: 2720–2736, 1999.

Hepp K, Van Opstal AJ, Straumann D, Hess BJ, Henn V. Monkey superior colliculus represents rapid eye movements in a two-dimensional motor map. *J Neurophysiol* 69: 965–979, 1993.

Keppel G, Wickens TD. *Design and Analysis: A Researcher's Handbook.* Old Tappan, NJ: Prentice Hall, 2004.

Klier EM, Wang H, Crawford JD. The superior colliculus encodes gaze commands in retinal coordinates. *Nat Neurosci* 4: 627–632, 2001.

Krommenhoek KP, Van Opstal AJ, Van Gisbergen JA. An analysis of craniocentric and oculocentric coding stages in a neural network model of the saccadic system. *Neural Networks* 9: 1497–1511, 1996.

Lee C, Rohrer WH, Sparks DL. Population coding of saccadic eye movements by neurons in the superior colliculus. *Nature* 332: 357–360, 1988.

Mays LE, Sparks DL. Saccades are spatially, not retinocentrically, coded. *Science* 208: 1163–1165, 1980.

McCluskey MK, Cullen KE. Eye, head, and body coordination during large gaze shifts in rhesus monkeys: movement kinematics and the influence of posture. *J Neurophysiol* 97: 2976–2991, 2007.

Miyashita N, Hikosaka O. Minimal synaptic delay in the saccadic output pathway of the superior colliculus studied in awake monkey. *Exp Brain Res* 112: 187–196, 1996.

Munoz DP, Wurtz RH. Saccade-related activity in monkey superior colliculus. I. Characteristics of burst and buildup cells. *J Neurophysiol* 73: 2313–2333, 1995.

Nagy B, Corneil BD. Representations of horizontal head-on-body position in the primate superior colliculus. *Soc Neurosci Abstr* 33: 178.12, 2007.

Paré M, Wurtz RH. Monkey posterior parietal cortex neurons antidromically activated from superior colliculus. *J Neurophysiol* 78: 3493–3497, 1997.

Paré M, Wurtz RH. Progression in neuronal processing for saccadic eye movements from parietal cortex area lip to superior colliculus. *J Neurophysiol* 85: 2545–2562, 2001.

Populin LC. Monkey sound localization: head-restrained versus head-unrestrained orienting. *J Neurosci* 26: 9820–9832, 2006.

Pouget A, Sejnowski TJ. Spatial transformations in the parietal cortex using basis functions. *J Cogn Neurosci* 9: 222–237, 1997.

Rezvani S, Corneil BD. Recruitment of a head turning synergy by low-frequency activity in the primate superior colliculus. *J Neurophysiol* 100: 397–411, 2008.

Richmond FJ, Abrahams VC. Morphology and distribution of muscle spindles in dorsal muscles of the cat neck. *J Neurophysiol* 38: 1322–1339, 1975.

Richmond FJ, Bakker DA. Anatomical organization and sensory receptor content of soft tissues surrounding upper cervical vertebrae in the cat. *J Neurophysiol* 48: 49–61, 1982.

Richmond FJ, Corneil BD. Afferent mechanisms in the upper cervical spine. In: *The Cranio-Cervical Syndrome: Mechanisms, Assessment and Treatment*, edited by Vernon H. Oxford, UK: Butterworth–Heinemann, 2001, p. 14–30.

Richmond FJ, Singh K, Corneil BD. Marked non-uniformity of fiber-type composition in the primate suboccipital muscle obliquus capitis inferior. *Exp Brain Res* 125: 14–18, 1999.

Robinson DA. Eye movements evoked by collicular stimulation in the alert monkey. *Vision Res* 12: 1795–1808, 1972.

Roll R, Velay JL, Roll JP. Eye and neck proprioceptive messages contribute to the spatial coding of retinal input in visually oriented activities. *Exp Brain Res* 85: 423–431, 1991.

Salinas E, Abbott LF. Coordinate transformations in the visual system: how to generate gain fields and what to compute with them. *Prog Brain Res* 130: 175–190, 2001.

Smith MA, Crawford JD. Distributed population mechanism for the 3-D oculomotor reference frame transformation. *J Neurophysiol* 93: 1742–1761, 2005.

Snyder LH, Grieve KL, Brotchie P, Andersen RA. Separate body- and world-referenced representations of visual space in parietal cortex. *Nature* 394: 887–891, 1998.

Sommer MA, Wurtz RH. Brain circuits for the internal monitoring of movements. *Annu Rev Neurosci* 31: 317–338, 2008.

Sparks D, Rohrer WH, Zhang Y. The role of the superior colliculus in saccade initiation: a study of express saccades and the gap effect. *Vision Res* 40: 2763–2777, 2000.

Sparks DL, Holland R, Guthrie BL. Size and distribution of movement fields in the monkey superior colliculus. *Brain Res* 113: 21–34, 1976.

Sparks DL, Mays LE. Spatial localization of saccade targets. I. Compensation for stimulation-induced perturbations in eye position. *J Neurophysiol* 49: 45–63, 1983.

Stanford TR, Freedman EG, Sparks DL. Site and parameters of microstimulation: evidence for independent effects on the properties of saccades evoked from the primate superior colliculus. *J Neurophysiol* 76: 3360–3381, 1996.

Taylor JL, McCloskey DI. Illusions of head and visual target displacement induced by vibration of neck muscles. *Brain* 114: 755–759, 1991.

Thompson KG, Hanes DP, Bichot NP, Schall JD. Perceptual and motor processing stages identified in the activity of macaque frontal eye field neurons during visual search. *J Neurophysiol* 76: 4040–4055, 1996.

Tollin DJ, Populin LC, Moore JM, Ruhland JL, Yin TC. Sound-localization performance in the cat: the effect of restraining the head. *J Neurophysiol* 93: 1223–1234, 2005.

Van Opstal AJ, Goossens HH. Linear ensemble-coding in midbrain superior colliculus specifies the saccade kinematics. *Biol Cybern* 98: 561–577, 2008.

Van Opstal AJ, Hepp K, Suzuki Y, Henn V. Influence of eye position on activity in monkey superior colliculus. *J Neurophysiol* 74: 1593–1610, 1995.

Vliegen J, Van Grootel TJ, Van Opstal AJ. Dynamic sound localization during rapid eye–head gaze shifts. *J Neurosci* 24: 9291–9302, 2004.

Vliegen J, Van Grootel TJ, Van Opstal AJ. Gaze orienting in dynamic visual double steps. *J Neurophysiol* 94: 4300–4313, 2005.

Volle M, Guitton D. Human gaze shifts in which head and eyes are not initially aligned. *Exp Brain Res* 94: 463–470, 1993.

Walton MM, Bechara B, Gandhi NJ. Role of the primate superior colliculus in the control of head movements. *J Neurophysiol* 98: 2022–2037, 2007.

Wurtz RH, Sommer MA, Paré M, Ferraina S. Signal transformations from cerebral cortex to superior colliculus for the generation of saccades. *Vision Res* 41: 3399–3412, 2001.

Xing J, Andersen RA. Models of the posterior parietal cortex which perform multimodal integration and represent space in several coordinate frames. *J Cogn Neurosci* 12: 601–614, 2000.

Zipser D, Andersen RA. A back-propagation programmed network that simulates response properties of a subset of posterior parietal neurons. *Nature* 331: 679–684, 1988.